Published in final edited form as:
Clin Exp Metastasis. 2011 April ; 28(4): 377–389. doi:10.1007/s10585-011-9377-9.

Effect of zoledronic acid and amputation on bone invasion and lung metastasis of canine osteosarcoma in nude mice

Tobie D. Wolfe, **Smitha Pankajavally Somanathan Pillai**, **Blake Eason Hildreth III**, **Lisa G. Lanigan**, **Chelsea K. Martin**, **Jillian L. Werbeck**, and **Thomas J. Rosol**
Department of Veterinary Biosciences, The Ohio State University, 1925 Coffey Road, Columbus, OH 43210, USA

Thomas J. Rosol: rosol.1@osu.edu

Abstract

Osteosarcoma (OSA) is an aggressive, highly metastatic and lytic primary bone neoplasm commonly affecting the appendicular skeleton of dogs and children. Current treatment options include amputation of the afflicted limb, limb-sparing procedures, or palliative radiation with or without adjunct chemotherapy. Therapies that inhibit bone resorption, such as the bisphosphonates, may be an effective palliative therapy by limiting the local progression of OSA in those patients that are not viable candidates for amputation. We have developed a mouse model of canine skeletal OSA following intratibial inoculation of OSCA40 cells that spontaneously metastasized to the lungs. We demonstrated that therapy with a nitrogen-containing bisphosphonate, zoledronic acid (Zol), reduced OSA-induced bone lysis; however, Zol monotherapy or in combination with amputation was not effective at inhibiting pulmonary metastasis. While not reaching statistical significance, amputation of the tumor-bearing limb reduced the average incidence of lung metastases; however, this effect was nullified when Zol was added to the treatment protocol. In untreated mice, the magnitude of proximal tibial lysis was significantly correlated with the incidence of metastasis. The data support amputation alone for the management of appendicular OSA rather than combining amputation with Zol. However, in patients that are not viable candidates for amputation, Zol may be a useful palliative therapy for OSA by reducing the magnitude of lysis and therefore bone pain, despite the risk of increased pulmonary metastasis.

Keywords

Canine; Osteosarcoma; Bone lysis; Metastasis; Nude mice; Zoledronic acid; Dog

Introduction

Osteosarcoma (OSA) is the most common primary bone tumor in both dogs and man [1, 2]. OSA most commonly arises in the appendicular skeleton and affected bones develop both

Correspondence to: Thomas J. Rosol, rosol.1@osu.edu.
Tobie D. Wolfe and Smitha Pankajavally Somanathan Pillai are the co-first authors and equally contributed to the work.

trabecular and cortical osteolysis. In addition to lysis, affected bones have variable degrees of reactive bone formation in both the endosteal and periosteal compartments, as well as osteoid formation by the tumor cells. Different histologic types of OSA have been recognized, including osteoblastic, chondroblastic, fibroblastic, anaplastic, telangectatic, giant-cell rich, and small cell variants [3]. Large breed dogs and adolescent children are most commonly affected and often develop pulmonary metastases. Despite the fact that OSA behaves and appears histologically similar in both species, it occurs more frequently in dogs than in man [4]. For these reasons, canine OSA is an ideal model to study the behavior of the disease process and to investigate treatment options for the management of both canine and human OSA.

In dogs afflicted with OSA, the appendicular skeleton is affected three to four times as often as the axial skeleton. Preferential sites include the metaphyseal region of the distal radius, proximal humerus, distal femur, and proximal tibia [5, 6]. Diagnostic radiography both raises the index of suspicion for OSA and assists in the clinical staging of the disease, particularly by indicating if late-stage pulmonary metastasis has occurred. Cortical bone lysis and a “sunburst” pattern of periosteal and endosteal new bone are radiographic hallmarks of the disease [1, 7–9]. While only 10% of cases present initially with radiographically evident pulmonary metastases, greater than 90% of dogs will develop pulmonary metastasis when treated with limb amputation alone [2, 10–12]. While all of these clinical and radiographic features are suggestive of OSA, definitive diagnosis is obtainable only by biopsy and histologic examination.

Amputation of the affected limb with or without adjuvant chemotherapy is currently the most common surgical procedure performed for OSA in dogs. However, limb-sparing procedures are receiving growing popularity [10, 11]. In the absence of chemotherapy, the average survival time in dogs receiving amputation alone is approximately 19 weeks [12]. Dogs typically are euthanized following amputation due to the morbidity associated with pulmonary metastasis, and less commonly, metastasis to additional organ systems or other locations in the appendicular or axial skeleton.

Inhibition of osteoclast-mediated resorption of bone at the site of the primary tumor may delay metastasis, thereby increasing survival times. The bisphosphonate class of drugs has been shown to have clinical utility in the management of solid bone tumors in dogs and man by decreasing bone lysis, thereby reducing skeletal complications and pain [13]. Of these, nitrogen-containing bisphosphonates, including Zol, have been shown to have antitumor activities and bone protective effects by reducing osteoclastic bone resorption and, to a lesser extent, promoting new bone formation [14, 15]. However, conflicting results have been reported in regard to the effects of Zol against OSA-induced pulmonary metastasis [15, 16].

The aim of this investigation was to develop a novel nude mouse model of canine skeletal OSA that would both develop a primary bone tumor at the site of inoculation (proximal tibial metaphysis) and spontaneously metastasize to the lungs. This model was used to study the effects of both amputation and the aminobisphosphonate, Zol, alone and in combination, on both the primary tumor and pulmonary metastasis.

Materials and methods

Cell lines and culture

Eleven canine OSA cell lines (OSCA 2, 8, 11M, 16, 21, 36, 39.1, 40, 50, 59.1 and D17) were generously donated from Dr. Jaime Modiano (University of Minnesota, College of Veterinary Medicine). Cells were grown in RPMI (Invitrogen Corp., Carlsbad, CA) and DMEM with 10% fetal bovine serum (FBS) and Primocin (Invitrogen Corp.). Cell lines were passaged at 80–90% confluence. All cell lines were tested for *Mycoplasma* spp. contamination by PCR using a primer set specific to the 16S rRNA coding region of the mycoplasma genome (VenorGem, Sigma-Aldrich, St. Louis, MO, USA). Cultures that contained *Mycoplasma* were treated with BM-Cyclin 1 and 2 according the manufacturer's instructions (Boehringer Mannheim, Mannheim, Germany) and retested by PCR.

Nude mouse experiments

Female nude mice (6-weeks-old) were obtained from Harlan Life Sciences (Indianapolis, IN). Mouse experiments were approved by The Ohio State University Institutional Laboratory Animals Care and Use Committee (Protocol No.: 2006A0119 and 2009A0099).

Pilot study

Osteosarcoma cell lines were injected subcutaneously into three nude mice per cell line to determine which cells would form viable xenografts in vivo. A total of 11 canine OSA cell lines from the Modiano laboratory were evaluated for engraftment. Nude mice were anesthetized with isoflurane (3%) with an induction chamber and maintained with a mask. Cells (10^5 cells in 100 μl of sterile PBS) were injected into the subcutis of the flank using a 22 gauge needle and 1 ml syringe. Tumor growth was observed for up to 12 weeks or until tumors were greater than 1 cm^3. Mice were euthanatized with 100% CO_2, tumors dissected, weighed, minced, washed with PBS, and either frozen (in DMEM Medium with 20% FBS, 10% DMSO, 1% L-glutamine, and Primocin), reinjected subcutaneously into additional nude mice (with or without Matrigel; 300 μl of PBS or 150 μl PBS/150 μl Matrigel, Sigma-Aldrich), or cultured in vitro. Tumor samples were also fixed in 10% neutral-buffered formalin, embedded in paraffin, sectioned, and stained with hematoxylin and eosin (H&E).

Intratibial injections

Osteosarcoma cell lines that formed tumors subcutaneously (OSCA21, 40, D17) were injected into the metaphysis of the tibia of nude mice to determine if the cells would form tumors in bone. Nude mice were anesthetized with isoflurane (3%). One hundred thousand (10^5) cells in 10–20 μl of sterile PBS were injected into the tibias of three nude mice each using a 25 gauge needle and Hamilton syringe. Mice were observed for up to 12 weeks or until early removal criteria were met (lameness, pain, swelling, inflammation, or greater than 10% weight loss). Mice were euthanatized with 100% CO_2, legs were radiographed, tibias were dissected, fixed in 10% neutral-buffered formalin for 48 h, decalcified in 10% EDTA (pH 7.4), embedded in paraffin, sectioned at 5 μm thickness, and stained with H&E.

Based on our preliminary results, the OSCA40 cell line, which engrafted both subcutaneously and intratibially, was chosen for further investigation. OSCA40 cells

originated from a 5.8-year-old, female, spayed St. Bernard that was diagnosed with a right distal femur OSA and treated only with amputation. The dog succumbed to metastatic disease 36 days following the initial diagnosis. The tumor was diagnosed by histopathology as an osteoblastic OSA.

Effects of zoledronic acid (Zol) and amputation

The effects of Zol (zoledronic acid, brand name Zometa®, Novartis, East Hanover, NJ) and amputation were measured in four groups of female nude mice (n = 12 per group) for 78 days. All four groups of mice received intratibial injections of OSCA40 cells (10^5 cells in 20 μl of sterile PBS) at the same time (day 0) in their right hindlimbs. The groups consisted of: Group 1 (saline and amputation), Group 2 (Zol and amputation), Group 3 (Zol alone), and Group 4 (saline alone). Mice that did not develop radiographic or histological evidence of engraftment were not included in the data analysis (1 from group 1, 2 from group 3, and 2 from group 4). Mice were examined daily and weighed twice weekly. Zol or saline (vehicle control) were injected subcutaneously (0.1 mg/kg in 200 μl PBS) twice per week starting on day 28. Right hind legs (containing the bone tumors) from mice in groups 1 and 2 were amputated by coxofemoral joint disarticulation between days 44 and 46. For amputations, anesthesia was induced with 5% isoflurane (IsoSol™, Vedco, Inc., St. Joseph, MO) and 2 l/min oxygen in an induction chamber and subsequently maintained with 1.5% isoflurane and 1 l/min oxygen. The tumor-inoculated hind limb was aseptically prepared with alternating scrubs of 100% ethanol and dilute chlorhexidine acetate (Pfizer Animal Health, New York, NY). A circumferential skin and subcutaneous fat incision was made with a number 15 scalpel blade at the level of the mid femur. The femoral artery and vein were concurrently ligated at the level of the mid-femur with ligating clips (Hemoclip®, Weck Closure Systems, Research Triangle Park, NC) and transected with scissors. Circumferential musculature was transected proximal to the level of vessel ligation and elevated from the femur to the level of the coxofemoral joint. The femoral neck and the remaining muscle attachments to the proximal femur were transected and the tumor-bearing limb removed. The remaining femoral head and neck were sharply excised. The acetabulum and sciatic nerve were blocked with 0.01 ml of 2% lidocaine (Lidoject®, IVX Animal Health, Inc., St. Joseph, MO). Musculature was closed over the acetabulum with 5-0 polyglyconate (Maxon®, Tyco Healthcare Group LP, Norwalk, CT) in an interrupted cruciate mattress pattern. The skin edges were apposed with a buried simple interrupted pattern and tissue adhesive (Vetbond™, 3M Corp., St. Paul, MN). Mice were recovered by discontinuation of isoflurane and maintenance on 1 l/min oxygen until ambulatory. The amputated legs were radiographed and fixed in formalin. Pre- and post-operative analgesia consisted of subcutaneous injection of 0.1 mg/kg buprenorphine (Buprenex®, Reckitt Benckiser Pharmaceuticals Inc., Richmond, VA) prior to surgery and every 8–12 h for 2 days after surgery. In addition, 0.3 mg/kg/day meloxicam (Metacam®, Boehringer Ingelheim Corp., Ridgefield, CT) and 31.5 mg/kg/day enrofloxacin (Baytril®, Bayer HealthCare, LLC, Shawnee Mission, KS) were added to the drinking water for 7 days after surgery. Mice were examined 2–3 times per day until the surgical sites were healed (up to day 10 post surgery).

All four groups of mice were euthanatized (with 100% CO2 and cervical dislocation) on day 78. Skin and muscle were removed from the hind legs with OSA and the legs were fixed in

formalin. The lungs were inflated by intratracheal instillation of 2–3 ml formalin. All lung lobes were embedded in paraffin and sections were stained with H&E. H&E-stained slides of cross-sections of all lung lobes were scanned at 400× using the Aperio Scanscope® CS slide scanner (Aperio Technologies, Vista, CA). The total lung area, size and number of metastases were measured using Aperio ImageScope viewing software (version 9.1.19.1569; Aperio Technologies, Vista, CA). The number of metastases and relative sizes were quantified using the H&E-stained sections. Metastases were classified into one of six sizes (1—<100 μm, 2—100 to 200 μm, 3—200 to 300 μm, 4—300 to 500 μm, 5—500 to 800 μm, 6—>800 μm). Based on these tumor sizes, relative tumor volumes were calculated for each size classification (Table 1). Within each size classification, the numbers of metastases were multiplied to these relative tumor volumes specific for each size classification and values summed to give a relative weighted tumor volume per mouse.

Immunohistochemistry

Vimentin immunohistochemistry was used to stain metastatic canine OSA cells in the lungs. The primary antibody for porcine vimentin is specific for large mammals including the dog, but does not cross-react with mouse vimentin. Immunohistochemistry for F4/80, CD45, CD3 and B220 was used to identify macrophages, leucocytes, T and B-cells, respectively, in the pulmonary metastases. Sections were deparaffinized, hydrated and pretreated with Target Retrieval Solution (DakoCytomation, Carpinteria, CA). The slides were then treated with 3% hydrogen peroxide solution for 10 min and blocked with serum-free protein. The slides were treated with primary antibody, rinsed with wash buffer followed by secondary antibody (Table 2). Color development was achieved using Vector RTU ABC Elite complex (Vector laboratories, Burlingame, CA) for 30 min, incubated with DAB substrate (DakoCytomation, Carpinteria, CA) for 5 min and counterstained with Hematoxylin.

Faxitron radiography

High resolution radiographic images of the tibias and femurs were obtained using a Faxitron cabinet X-ray system (Hewlett-Packard, McMinnville, OR) using Kodak film (Eastman Kodak, Rochester, New York) at 45 kVp for 3.5 min. The radiographs were scanned at 1,800 dots per inch. Areas of tibial bone lysis and proximal tibial area were measured using Image Pro plus version 5.0 software (Media Cybernetics, Silver Spring, MD) and data were presented as percent lysis of bone area. The effects of Zol on bone in vivo were measured in mice that successfully developed xenografts after intratibial injections.

Bone histology

Formalin-fixed bones were decalcified with 10% EDTA (for up to 2 weeks at 4°C) on a shaker platform, embedded in paraffin, sectioned, and stained with H&E and tartrate-resistant acid phosphatase (TRAP) (Acid Phosphatase Kit 387-A; Sigma Diagnostics, St. Louis, MO) to identify active osteoclasts. TRAP staining was performed on non-stained sections that were deparaffinized using 3–5 min washes with xylene (Hemo-De, Fisher Scientific, and Bay Shore, NY) and rehydrated in decreasing concentrations of ethanol (100, 95, 80, 70 and finally 50%). For staining of TRAP, antigen retrieval on the sections was performed using heat treatment at 95 °C for 20 min in preheated antigen retrieval solution (DakoCytomation) and then stained for TRAP. The slides were counterstained with

hematoxylin. The distribution and morphology of large, active osteoclasts (TRAP-positive osteoclasts with three or more nuclei) were examined at the metaphyses of the tumor-bearing tibia and at the bone-tumor interface.

Data analysis and statistics

Results are displayed as mean ± standard error of the mean (SEM). Outlier screening was initially performed within each treatment group using the Grubb's test for each outcome variable. If identified, a maximum of two outlier mice were removed per treatment group. Data distribution and variance were subsequently analyzed. All data were normally distributed, except relative weighted tumor volume, which assumed a normal distribution following square root transformation. This allowed for all comparisons to be conducted with parametric unpaired *t* tests unless otherwise stated. Welch's correction was performed if groups had unequal variances. Percent bone lysis of the proximal tibia was compared between saline and Zol-treated mice at the time of amputation and at the time of euthanasia in mice not receiving amputation. Percent change in body weight from the time of (1) intratibial injection to amputation; (2) intratibial injection to euthanasia in mice not receiving amputation; and (3) amputation to euthanasia were compared between saline and Zol-treated mice. The incidence of metastasis and relative weighted tumor volume normalized to lung volume were compared between (1) saline and Zol-treated mice not receiving amputation; (2) saline and Zol-treated mice receiving amputation; and (3) saline treated mice receiving and not receiving amputation. The correlation between percent bone lysis of the proximal tibia and both the incidence of metastasis and the relative weighted tumor volume was assessed for all treatment groups using Pearson's correlation analysis. All analyses were performed with Prism ver. 5.00 (GraphPad Software, Inc., San Diego, CA) with the level of statistical significance established at $P < 0.05$. Due to our interest in only select comparisons between treatment groups in regards to incidence of metastasis and relative weighted tumor volume, the adjusted threshold for statistical significance was $P < 0.017$, which allowed for multiple comparisons to be executed with an unpaired *t* test.

Results

Pilot study for subcutaneous tumor growth (all cell lines)

Three of the 11 evaluated cell lines (OSCA 21, 40, D17) produced viable subcutaneous tumors in nude mice. The experiment was terminated at week 10. The average tumor volume was calculated by the formula, $v = 1/2 \times \text{Length} \times \text{Width} \times \text{Height}$ [17]. The approximate tumor volume for OSCA21 was 100 mm^3, OSCA40 was 30 mm^3, and D17 was 500 mm^3. Histopathology of the tumors demonstrated that they were composed of anaplastic spindle cells with oval elongated nuclei, with single prominent nucleoli and scant to moderate lightly eosinophilic to amphophilic cytoplasm. The cells showed moderate anisocytosis and anisokaryosis, with occasional neoplastic syncytia. The OSCA40 cells invaded muscle with evidence of muscle necrosis. None of the tumors produced osteoid.

Subsequent subcutaneous injection of the OSCA40, 21, and D17 cell lines in combination with Matrigel into three mice per cell line did not increase the rate of tumor growth or alter tumor morphology.

Pilot study for intratibial tumor growth (OSCA40, OSCA21, and D17 cells)

All OSCA40 injected mice (n = 3) developed metaphyseal OSA and multiple lung metastases. None of the mice injected with OSCA21 or D17 cells developed intratibial tumors. Visible soft tissue swelling was noted around the injection site in proximal tibia from the 4th week in OSCA40 group. Radiography demonstrated lysis of both cortical and medullary bone with evidence of surrounding soft tissue swelling. Histopathology of the tumors demonstrated that they were composed of anaplastic spindle shaped cells with oval elongated nuclei with scant to moderate amounts of lightly eosinophilic to amphophilic cytoplasm. The neoplastic cells had moderate anisocytosis and anisokaryosis and moderate numbers of mitotic figures were present (2–3 per 40× field). There was aggressive bone lysis of the proximal tibia with evidence of invasion across the stifle joint into the distal femur. Metastases were present only in the lungs based on gross necropsy findings of the heart, liver, kidneys, spleen, brain and lymph nodes.

General anesthesia and hindlimb amputation

All mice that received intratibial inoculation of OSCA40 cells and were subjected to amputation underwent induction, maintenance, and recovery from general anesthesia uneventfully at the time of surgery. There were no intraoperative or post-operative surgical complications, with all surgical skin incisions healing completely within 10 days in both saline and Zol-treated mice.

Effect of Zol on proximal tibial osteolysis

OSCA40 cells inoculated intratibially into nude mice successfully engrafted and produced tumors in the proximal tibia. Radiographic images of tumor-bearing tibias confirmed osteolysis, which was characterized by the loss of cortical and medullary bone in both the metaphysis and proximal diaphysis in saline-treated and Zol-treated mice. At the time of amputation (6 weeks post-intratibial injection), treatment with Zol for 2 weeks had no effect on the percent lysis of the proximal tibia when compared to saline treated mice (24 ±3.1 vs. 28 ± 6.5%, respectively, P = 0.553, Fig. 1a). However, in non-amputated mice, treatment with Zol resulted in a statistically significant decrease in percent lysis of the proximal tibia induced by OSCA40 cells at week 11 (18 ± 3.8%) when compared to mice treated with saline alone (48 ± 12%, P = 0.036, Fig. 1b). In the Zol-treated group, there was intact cortical bone with mild metaphyseal osteolysis, demonstrating that Zol inhibited osteolysis when compared to saline (Fig. 1c, d).

In order to evaluate the global skeletal effects of Zol, contralateral tibias (non-tumor-bearing) were radiographed. Zol treatment increased the radiopacity of the proximal tibial metaphysis when compared to saline-treated mice (Fig. 2a). This radiographic feature demonstrated increased bone density resulting from the inhibition of osteolysis of the metaphyseal primary spongiosa. The increase in bone density in Zol-treated mice correlated histologically to an increase in trabecular number and thickness within the primary spongiosa (Fig. 2b). The radiographic and histologic findings confirm the in vivo efficacy of Zol.

Histopathology of intratibial osteosarcoma with OSCA40 cells

Osteosarcomas grew in the epiphysis, metaphysis and proximal diaphysis of tibias injected with the OSCA40 cells. The OSAs induced both trabecular and cortical bone lysis and secondary periosteal new bone formation. Histologically, the tumors were composed of spindle to polyhedral cells with oval elongated nuclei, scant to moderate amounts of lightly eosinophilic cytoplasm. The cells showed moderate anisocytosis and anisokaryosis (Fig. 3a). Moderate numbers of mitotic figures (2–3 per 40× field) were observed. Multinucleated tumor cells were also present. Multifocal mild hemorrhage and necrosis were observed within some of the large tumor masses.

In tumor-bearing tibias, Zol inhibited bone resorption, which was characterized by a reduction in the magnitude of trabecular and cortical bone loss. In addition, new woven bone formation occurred adjacent to the tumor cells in both the metaphysis and proximal diaphysis (Fig. 3a). TRAP-stained bone sections were used to assess the effect of Zol on osteoclast number and activity at the tumor-bone interface. Numerous TRAP-positive osteoclasts were present along the tumor-bone interface in both vehicle- and Zol-treated mice (Fig. 3b). No differences were observed in the number of osteoclasts between vehicle- and Zol-treated mice in both tumor-bearing limbs and in contra-lateral non-injected limbs. However, the osteoclasts from Zol-treated mice were large with many nuclei and cytoplasmic vacuolation in both tumor-bearing limbs and contralateral non-injected limbs (Fig. 3b). This vacuolation was interpreted as osteoclast degeneration, suggesting that Zol impaired osteoclast function.

Body weight in mice with intratibial injection of OSCA40 cells

Body weights of the four groups of mice were measured once weekly to determine the effects of Zol on body weight. Treatment with Zol had no effect on body weight at the time of amputation and at the end of the study in both amputated and non-amputated mice (P ranging from 0.226 to 0.922).

Lung metastases in mice with intratibial injection of OSCA40 cells

Mice that were injected intratibially with OSCA40 cells developed widespread multifocal lung metastases ranging from 50 to 2,000 μm in diameter (Fig. 4). Smaller metastases grew in the alveolar walls forming a radiating pattern. As the metastases became larger, they formed solid masses with areas of central necrosis. Some metastases were present in vessels with fibrin thrombi, adjacent to bronchioles, or were subpleural. Larger metastases had prominent inflammation that was concentrated at the periphery of the tumors. Neoplastic cells were large with marked anisocytosis and anisokaryosis. Nuclei were round or oval with finely stippled chromatin. Some of the nuclei had large nucleoli. Cell margins were indistinct and few mitoses were present. Using immunohistochemistry, OSCA40 cells stained strongly positive for vimentin and there was no staining of normal mouse lung or mouse inflammatory cells with the vimentin primary antibody, which confirmed that the metastatic cells were canine in origin (Fig. 5a). All inflammatory cells in the metastases had strong immunoreactivity for a mouse pan-leucocyte marker (CD45), a small number of these cells had reactivity for a macrophage marker (F4/80), and a large number of these cells had immunoreactivity for a B-cell marker (B220), with the B cells forming multifocal small

aggregates at the periphery of the tumors (Fig. 5b – d). Rare leukocytes had immunoreactivity for a mouse T-cell marker (CD3) (Fig. 5e).

Effect of amputation and Zol on lung metastases

The incidence of metastases in the four treatment groups, classified based on the size of the individual metastases, is shown in Table 3. Amputation reduced the average incidence of metastasis when compared to saline alone or combined Zol and amputation; however, the difference did not reach statistical significance ($P = 0.154$ and 0.125, adjusted threshold for significance $P < 0.017$) (Fig. 6a). In non-amputated mice, Zol had no effect on the incidence of metastasis ($P = 0.342$).

Despite an increase in average relative weighted tumor volume following Zol treatment in non-amputated mice ($P = 0.122$, adjusted threshold for significance $P < 0.017$) (Fig. 6b), there were no statistically significant differences between treatment groups.

In non-amputated mice treated with saline, there was a significant correlation between the magnitude of proximal tibial lysis and the incidence of metastasis ($R^2 = 0.923$, $P = 0.0001$, Fig. 7a) and the correlation between bone lysis and the relative weighted tumor volume of lung metastases approached statistical significance ($R^2 = 0.465$, $P = 0.063$). In contrast, there was no correlation within the remaining treatment groups between proximal tibial lysis and either the incidence of metastasis or the relative weighted tumor volume.

Discussion

Appendicular OSA represents between 80 and 90% of malignant bone tumors in both dogs and man and frequently metastasizes to the lungs [18]. Investigation of new therapeutics for this debilitating and often fatal neoplasm initially requires the development of relevant in vitro and in vivo models that mimic tumor biology, progression, and the metastatic cascade [19, 20]. Syngeneic and xenograft mouse models of OSA have been established for this reason [15, 21–23]. Canine OSA is highly comparable to its human counterpart in regards to its molecular, histologic, and radiographic characteristics, as well as its high metastatic rate in both species [24, 25]. Therefore, canine OSA is an ideal model to study the progression and treatment of human OSA.

We have created a skeletal xenograft nude mouse model of canine OSA. In our model, OSCA40 engrafted in the proximal tibia, producing primary bone tumors that spontaneously metastasized to the lungs. The OSCA40 cells caused histologic and radiologic evidence of osteolysis in the metaphysis and proximal diaphysis of the tibia. OSA cell lines with osteoblastic and mixed osteoblastic-osteolytic phenotypes have been previously established [26–28]. The pathogenesis of OSA and local bone lysis are poorly understood. The progression of OSA in bone has been associated with a vicious cycle where products of bone lysis stimulate tumor proliferation, after which the tumor secretes factors that stimulate osteoclasts to resorb bone [29–31]. Bone destruction may have resulted from the upregulation of several osteolytic mediators, including IL-1, IL-6, IL-8 and receptor activator of NFkB (RANK) by OSCA40 cells and subsequent stimulation of osteoclasts

[31]. Therefore, suppressing bone lysis by inhibiting osteoclast activity will not only decrease bone destruction, but may potentially prevent primary tumor progression.

We used the nitrogen-containing bisphosphonate, Zol, which has been shown to be a potent inhibitor of osteoclasts and tumor growth in a variety of solid tumors [14, 32–35]. Nitrogen-containing bisphosphonates, such as Zol interfere with the mevalonate pathway by inhibiting farnesyl pyrophosphate synthase [36]. Inhibition of this pathway leads to reduced prenylation of small GTP-binding proteins which are involved in osteoclast function [37]. In addition, Zol has been shown to increase the in vitro expression of the osteoclast inhibitor, osteoprotegerin (OPG), in osteoblasts [38]. We hypothesized that inhibiting osteoclastic bone resorption with Zol would not only reduce bone loss, but would also inhibit OSA xenograft growth and potentially metastasis by inhibiting the vicious cycle.

In our study, Zol significantly reduced proximal tibial lysis after 7 weeks of treatment. This effect was not observed following only 2 weeks of treatment, indicating that this effect was time-dependent. We did not use histomorphometry to quantify cortical and trabecular bone in the proximal tibia since the tumors were at an advanced stage at the time of euthanasia with marked loss of trabecular and cortical bone. Future studies will use microCT analysis to more accurately measure cortical and trabecular bone volume and microarchitecture. In Zol-treated mice, osteoclasts continued to form since numerous osteoclasts were observed within the tumor and at the tumor-bone interface following 7 weeks of treatment in the tibias of Zol- and saline-treated mice. However, Zol inhibited osteoclastic bone resorption by inhibiting osteoclast function. In addition, in Zol-treated mice, there was evidence of osteoclast degeneration, which was demonstrated by cytoplasmic vacuoles. The precise mechanism of this vacuolar degeneration is not known; however, targeted inhibition of the small GTPase, Rab, resulted in reduced osteoclast function accompanied by dome-shaped cell morphology and large intracellular vacuoles [39]. It has also been postulated that inhibition of bone resorption caused a reduction of both local calcium concentrations and apoptotic signals in osteoclasts, leading to an increase in the duration of survival and more time for fusion of osteoclasts with mononuclear progenitors [40]. The cytoplasmic vacuoles as well as fusion with mononuclear progenitors may have contributed to the larger size of osteoclasts observed in Zol-treated mice. In addition to inhibiting bone resorption, we observed new woven bone within the medullary canal in Zol-treated mice. It has been shown that Zol is incorporated into new bone at higher rates than at quiescent surfaces [41]. The incorporation of Zol in bone as it is being formed may result in an osteoprotective effect. The effect of Zol is more pronounced in areas of rapid bone turnover, as observed in the proximal metaphyses. This was also evident on the contralateral non-tumor bearing tibias, which showed both histologic and radiographic evidence of increased thickness and number of the primary spongiosa.

Previous studies have reported that Zol had antitumor effects by inhibiting cancer cell adhesion, invasion and angiogenesis [42, 43]. In contrast, it has been reported with OSA (or other tumors) that there was a lack of efficacy of Zol against intratibial tumors [15, 44]. We did not observe a reduced tumor burden within the proximal tibia following Zol therapy even though it was administered for 7 weeks, despite the decrease in proximal tibial lysis. In addition, large tumors with areas of central necrosis were seen in both saline and Zol-treated

groups. The ability to measure the effect of Zol on OSA tumor growth in intratibial tumors is complicated by the Zol-mediated reduction in bone lysis, which would be expected to limit primary tumor growth by reducing invasion and growth outside of the tibia. We suggest that a subcutaneous OSA xenograft may be a more appropriate model to measure the effects of Zol specifically on primary tumor growth; however, this model would not be representative of the clinical manifestation of skeletal OSA.

In our study, we selected a dose of 0.1 mg/kg Zol twice weekly. This correlated to a human equivalent dose of 0.02 mg/kg weekly (when the human:mouse dosage conversion factor of 12.3 is used as recommended by the FDA). Currently, Zometa® is recommended by the manufacturer to be administered at a dosage of 4 mg, either once weekly for the management of humeral hypercalcemia of malignancy or once every 3 weeks for the treatment of multiple myeloma and skeletal metastases from solid tumors. When administered to a 60 kg individual, this would result in a weekly dosage of 0.07 or 0.02 mg/kg, respectively. Therefore, our weekly dose was equivalent to, or lower than, dosages currently recommended for human cancer patients. We have previously shown that this dosage is not only well-tolerated in mice, but also decreased osteolysis induced by multiple tumor types other than OSA, which was consistent with our findings in the present study [45–47]. We believe that while higher doses of Zol might have potentially elicited greater anti-tumor effects, it may have induced unwanted side effects, including mandibular osteonecrosis or renal failure [48, 49].

Metastasis of OSA to the lungs is associated with poor survival. This OSA model spontaneously metastasized to the lungs, allowing us to measure the effects of different treatments on metastasis. Amputation of the tumor-bearing hind limb resulted in a reduction in the average incidence of lung metastases; however, this decrease was not statistically significant. A previous report documented that surgical removal of the tumor up to 2 weeks following injection of tumor cells, but not later, prevented lung metastasis, suggesting that local tumor growth and invasion for a duration of at least 2 weeks is required for tumor metastasis [22]. In addition, in a mouse model of spontaneous OSA using luciferase imaging, lung metastases were detected 38 days following intratibial injections of OSA cells [23]. We amputated the hind legs 4-weeks following intratibial tumor cell inoculation, which permitted adequate time for the development of lung metastases. Clinically, it has been shown that dogs with smaller primary OSA have a better long-term prognosis when compared to dogs with larger tumors [50]. The improved prognosis is likely a result of prompt treatment at the time of an early diagnosis, before the development of a significant number of pulmonary metastases. We found a significant correlation between the magnitude of proximal tibial lysis and the incidence of metastasis in saline-treated non-amputated mice that supports amputation at the earliest detection of radiographic lysis. Early detection and amputation may prevent or delay the development of lung metastases, thereby reducing morbidity and ultimately improving survival.

The results from this study show that Zol failed to prevent lung metastasis, and may have enhanced both the incidence and size of metastases. There has been conflicting results reported on the effects of Zol on pulmonary metastasis in OSA. Zol was shown to have no effect or increase the incidence of pulmonary metastases using different models of OSA

[32]. However, it has also been reported that Zol inhibited or reduced the incidence of pulmonary metastases induced by OSA [16, 43, 51]. These differences likely result from the use of different animal models (rats/mice; syngeneic/xenograft), cell lines, dosage and treatment schedules of Zol, and potentially altered interactions of tumor cells with the hosts in these different models. More specifically, the importance of the immune system in mediating anti-tumor effects of Zol must be considered. Zol has been shown to stimulate gamma-delta T-cells to secrete pro-inflammatory cytokines that cause the death of cancer cells in vitro [32, 52]. Similarly, severe combined immunodeficiency mice reconstituted with human peripheral blood lymphocytes or purified gamma delta T cells have reduced tumor burden [53]. Nude mice, which lack T-cells, might potentially account for the lack of efficacy of Zol against the primary and metastatic tumor burden. Interestingly, there were prominent B-cells and macrophages within the lung metastases. It is possible that the inflammatory cells present within the metastases, either recruited by the host or tumor, may have played a role in metastasis growth.

In conclusion, we have created a nude mouse model of canine skeletal OSA that spontaneously metastasizes to the lungs. We demonstrated that Zol therapy reduced OSA-induced bone lysis; however Zol alone or in combination with amputation, was not effective at inhibiting pulmonary metastases. We suggest that amputation alone be elected for the management of appendicular OSA rather than combining amputation with Zol therapy. However, in patients that are not viable candidates for amputation, Zol may be a useful palliative therapy for OSA by reducing the magnitude of lysis and therefore bone pain, despite the risk of increased pulmonary metastasis.

Acknowledgments

The authors thank Dr. Jaime Modiano, Dr. Laura J. Rush, Alicia R. Montgomery; Dr. Bill C. Kisseberth; Dr. Matthew J. Allen; Alan Flechtner; and Dr. Wessel Dirksen for their help and technical support during the study.

References

1. Dorfman SK, Hurvitz AI, Patnaik AK. Primary and secondary bone tumours in the dog. J Small Anim Pract. 1977; 18:313–326. [PubMed: 267798]
2. Evans LB. Osteosarcoma in a young Great Dane dog. J S Afr Vet Assoc. 1983; 54:271–273. [PubMed: 6583421]
3. Chun R, de Lorimier LP. Update on the biology and management of canine osteosarcoma. Vet Clin N Am Small Anim Pract. 2003; 33:491–516.
4. Withrow SJ, Powers BE, Straw RC, Wilkins RM. Comparative aspects of osteosarcoma. Dog versus man. Clin Orthop Relat Res. 1991; 270:159–168. [PubMed: 1884536]
5. Spiers FW, Beddoe AH. Sites of incidence of osteosarcoma in the long bones of man and the beagle. Health Phys. 1983; 44(Suppl 1):49–64. [PubMed: 6575001]
6. Brodey RS, Fidler IJ, Bech-Nielsen S. Correlation of in vitro immune response with clinical course of malignant neo-plasia in dogs. Am J Vet Res. 1975; 36:75–80. [PubMed: 1054221]
7. Enneking WF. Editorial: Osteosarcoma. Clin Orthop Relat Res. 1975; 111:2–4. [PubMed: 1057463]
8. Liptak JM, Dernell WS, Straw RC, Rizzo SA, Lafferty MH, Withrow SJ. Proximal radial and distal humeral osteosarcoma in 12 dogs. J Am Anim Hosp Assoc. 2004; 40:461–467. [PubMed: 15533966]
9. Ebata K. Diagnostic imaging of skeletal disorders, with special reference to systemic diagnosis of malignant bone tumors. Nippon Ika Daigaku Zasshi. 1982; 49:601–608. [PubMed: 6216266]

10. Liptak JM, Pluhar GE, Dernell WS, Withrow SJ. Limb-sparing surgery in a dog with osteosarcoma of the proximal femur. Vet Surg. 2005; 34:71–77. [PubMed: 15720600]
11. Ehrhart N. Longitudinal bone transport for treatment of primary bone tumors in dogs: technique description and outcome in 9 dogs. Vet Surg. 2005; 34:24–34. [PubMed: 15720593]
12. Spodnick GJ, Berg J, Rand WM, Schelling SH, Couto G, Harvey HJ, Henderson RA, MacEwen G, Mauldin N, McCaw DL. Prognosis for dogs with appendicular osteosarcoma treated by amputation alone: 162 cases (1978–1988). J Am Vet Med Assoc. 1992; 200:995–999. [PubMed: 1577656]
13. Spugnini EP, Vincenzi B, Caruso G, Baldi A, Citro G, Santini D, Tonini G. Zoledronic acid for the treatment of appendicular osteosarcoma in a dog. J Small Anim Pract. 2009; 50:44–46. [PubMed: 18793253]
14. Coleman RE. Bisphosphonates: clinical experience. Oncologist. 2004; 9(Suppl 4):14–27. [PubMed: 15459426]
15. Labrinidis A, Hay S, Liapis V, Ponomarev V, Findlay DM, Evdokiou A. Zoledronic acid inhibits both the osteolytic and osteoblastic components of osteosarcoma lesions in a mouse model. Clin Cancer Res. 2009; 15:3451–3461. [PubMed: 19401351]
16. Ory B, Heymann MF, Kamijo A, Gouin F, Heymann D, Redini F. Zoledronic acid suppresses lung metastases and prolongs overall survival of osteosarcoma-bearing mice. Cancer. 2005; 104:2522–2529. [PubMed: 16270320]
17. Tomayko MM, Reynolds CP. Determination of subcutaneous tumor size in athymic (nude) mice. Cancer Chemother Pharmacol. 1989; 24:148–154. [PubMed: 2544306]
18. Bacci G, Avella M, Picci P, Briccoli A, Dallari D, Campanacci M. Metastatic patterns in osteosarcoma. Tumori. 1988; 74:421–427. [PubMed: 3055577]
19. de Santos LA, Edeiken B. Purely lytic osteosarcoma. Skeletal Radiol. 1982; 9:1–7. [PubMed: 6961529]
20. Pelfrene AF. A search for a suitable animal model for bone tumors: a review. Drug Chem Toxicol. 1985; 8:83–99. [PubMed: 3926448]
21. Crnalic S, Hakansson I, Boquist L, Lofvenberg R, Brostrom LA. A novel spontaneous metastasis model of human osteosarcoma developed using orthotopic transplantation of intact tumor tissue into tibia of nude mice. Clin Exp Metastasis. 1997; 15:164–172. [PubMed: 9062393]
22. Berlin O, Samid D, Donthineni-Rao R, Akeson W, Amiel D, Woods VL Jr. Development of a novel spontaneous metastasis model of human osteosarcoma transplanted orthotopically into bone of athymic mice. Cancer Res. 1993; 53:4890–4895. [PubMed: 8402677]
23. Miretti S, Roato I, Taulli R, Ponzetto C, Cilli M, Olivero M, Di Renzo MF, Godio L, Albini A, Buracco P, Ferracini R. A mouse model of pulmonary metastasis from spontaneous osteosarcoma monitored in vivo by luciferase imaging. PLoS One. 2008; 3:e1828. [PubMed: 18350164]
24. Selvarajah GT, Kirpensteijn J, van Wolferen ME, Rao NA, Fieten H, Mol JA. Gene expression profiling of canine osteosarcoma reveals genes associated with short and long survival times. Mol Cancer. 2009; 8:72. [PubMed: 19735553]
25. Parodi AL. Canine osteosarcoma as a model in comparative oncology. Sem Hop. 1982; 58:1731–1735. [PubMed: 6291155]
26. Yuan J, Ossendorf C, Szatkowski JP, Bronk JT, Maran A, Yaszemski M, Bolander ME, Sarkar G, Fuchs B. Osteoblastic and osteolytic human osteosarcomas can be studied with a new xenograft mouse model producing spontaneous metastases. Cancer Invest. 2009; 27:435–442. [PubMed: 19212826]
27. Ilaslan H, Schils J, Nageotte W, Lietman SA, Sundaram M. Clinical presentation and imaging of bone and soft-tissue sarcomas. Cleve Clin J Med. 2010; 77(Suppl 1):S2–S7. [PubMed: 20179183]
28. Tebbi CK, Gaeta J. Osteosarcoma. Pediatr Ann. 1988; 17:285–300. [PubMed: 3290815]
29. Lamoureux F, Richard P, Wittrant Y, Battaglia S, Pilet P, Trichet V, Blanchard F, Gouin F, Pitard B, Heymann D, Redini F. Therapeutic relevance of osteoprotegerin gene therapy in osteosarcoma: blockade of the vicious cycle between tumor cell proliferation and bone resorption. Cancer Res. 2007; 67:7308–7318. [PubMed: 17671200]

30. Lamoureux F, Trichet V, Chipoy C, Blanchard F, Gouin F, Redini F. Recent advances in the management of osteosarcoma and forthcoming therapeutic strategies. Expert Rev Anticancer Ther. 2007; 7:169–181. [PubMed: 17288528]
31. Lamoureux F, Picarda G, Rousseau J, Gourden C, Battaglia S, Charrier C, Pitard B, Heymann D, Redini F. Therapeutic efficacy of soluble receptor activator of nuclear factor-kappa B-Fc delivered by nonviral gene transfer in a mouse model of osteolytic osteosarcoma. Mol Cancer Ther. 2008; 7:3389–3398. [PubMed: 18852142]
32. Labrinidis A, Hay S, Liapis V, Findlay DM, Evdokiou A. Zoledronic acid protects against osteosarcoma-induced bone destruction but lacks efficacy against pulmonary metastases in a syngeneic rat model. Int J Cancer. 2010; 127:345–354. [PubMed: 19924813]
33. Kimura K, Nakano T, Park YB, Tani M, Tsuda H, Beppu Y, Moriya H, Yokota J. Establishment of human osteosarcoma cell lines with high metastatic potential to lungs and their utilities for therapeutic studies on metastatic osteosarcoma. Clin Exp Metastasis. 2002; 19:477–485. [PubMed: 12405284]
34. Body JJ. Bisphosphonates for malignancy-related bone disease: current status, future developments. Support Care Cancer. 2006; 14:408–418. [PubMed: 16450087]
35. Gatien M, Benjamin O, Berengere G, Franck V, Francois G, Frederic B, Francoise R, Dominique H. Therapeutic approach of primary bone tumours by bisphosphonates. Curr Pharm Des. 2010; 16:2981–2987. [PubMed: 20722622]
36. Kavanagh KL, Guo K, Dunford JE, Wu X, Knapp S, Ebetino FH, Rogers MJ, Russell RG, Oppermann U. The molecular mechanism of nitrogen-containing bisphosphonates as antiosteoporosis drugs. Proc Natl Acad Sci USA. 2006; 103:7829–7834. [PubMed: 16684881]
37. Hall A, Nobes CD. Rho GTPases: molecular switches that control the organization and dynamics of the actin cytoskeleton. Philos Trans R Soc Lond B Biol Sci. 2000; 355:965–970. [PubMed: 11128990]
38. Yuasa T, Kimura S, Ashihara E, Habuchi T, Maekawa T. Zoledronic acid - a multiplicity of anti-cancer action. Curr Med Chem. 2007; 14:2126–2135. [PubMed: 17691952]
39. Coxon JP, Oades GM, Kirby RS, Colston KW. Zoledronic acid induces apoptosis and inhibits adhesion to mineralized matrix in prostate cancer cells via inhibition of protein prenylation. BJU Int. 2004; 94:164–170. [PubMed: 15217454]
40. Weinstein RS, Roberson PK, Manolagas SC. Giant osteoclast formation and long-term oral bisphosphonate therapy. N Engl J Med. 2009; 360:53–62. [PubMed: 19118304]
41. Kimmel DB. Mechanism of action, pharmacokinetic and pharmacodynamic profile, and clinical applications of nitrogen-containing bisphosphonates. J Dent Res. 2007; 86:1022–1033. [PubMed: 17959891]
42. Guise TA. Antitumor effects of bisphosphonates: promising preclinical evidence. Cancer Treat Rev. 2008; 34(Suppl 1):S19–S24. [PubMed: 18486348]
43. Dass CR, Choong PF. Zoledronic acid inhibits osteosarcoma growth in an orthotopic model. Mol Cancer Ther. 2007; 6:3263–3270. [PubMed: 18089720]
44. Buijs JT, Que I, Lowik CW, Papapoulos SE, van der Pluijm G. Inhibition of bone resorption and growth of breast cancer in the bone microenvironment. Bone. 2009; 44:380–386. [PubMed: 19041433]
45. Shu ST, Nadella MV, Dirksen WP, Fernandez SA, Thudi NK, Werbeck JL, Lairmore MD, Rosol TJ. A novel bioluminescent mouse model and effective therapy for adult T-cell leukemia/lymphoma. Cancer Res. 2007; 67:11859–11866. [PubMed: 18089816]
46. Thudi NK, Martin CK, Prasad MVP, Fernandez SA, Werbeck JL, Pinzone JJ, Rosol TJ. Zoledronic acid decreased osteolysis but not bone metastasis in a nude mouse model of canine prostate cancer with mixed bone lesions. Prostate. 2008; 68:1116–1125. [PubMed: 18461562]
47. Martin CK, Werbeck JL, Thudi NK, Lanigan LG, Wolfe TD, Toribio RE, Rosol TJ. Zoledronic acid reduces bone loss and tumor growth in an orthotopic xenograft model of osteolytic oral squamous cell carcinoma. Cancer Res. 2010; 70:8607–8616. [PubMed: 20959474]
48. Edwards BJ, Gounder M, McKoy JM, Boyd I, Farrugia M, Migliorati C, Marx R, Ruggiero S, Dimopoulos M, Raisch DW, Singhal S, Carson K, Obadina E, Trifilio S, West D, Mehta J, Bennett

CL. Pharmacovigilance and reporting oversight in US FDA fast-track process: bisphosphonates and osteonecrosis of the jaw. Lancet Oncol. 2008; 9:1166–1172. [PubMed: 19038763]

49. Guise TA. Bone loss and fracture risk associated with cancer therapy. Oncologist. 2006; 11:1121–1131. [PubMed: 17110632]
50. Bacon NJ, Ehrhart NP, Dernell WS, Lafferty M, Withrow SJ. Use of alternating administration of carboplatin and doxorubicin in dogs with microscopic metastases after amputation for appendicular osteosarcoma: 50 cases (1999–2006). J Am Vet Med Assoc. 2008; 232:1504–1510. [PubMed: 18479240]
51. Koto K, Horie N, Kimura S, Murata H, Sakabe T, Matsui T, Watanabe M, Adachi S, Maekawa T, Fushiki S, Kubo T. Clinically relevant dose of zoledronic acid inhibits spontaneous lung metastasis in a murine osteosarcoma model. Cancer Lett. 2009; 274:271–278. [PubMed: 18986762]
52. Kurzman ID, Shi F, Vail DM, MacEwen EG. In vitro and in vivo enhancement of canine pulmonary alveolar macrophage cytotoxic activity against canine osteosarcoma cells. Cancer Biother Radiopharm. 1999; 14:121–128. [PubMed: 10850295]
53. Kabelitz D, Wesch D, Pitters E, Zoller M. Characterization of tumor reactivity of human V gamma 9V delta 2 gamma delta T cells in vitro and in SCID mice in vivo. J Immunol. 2004; 173:6767–6776. [PubMed: 15557170]

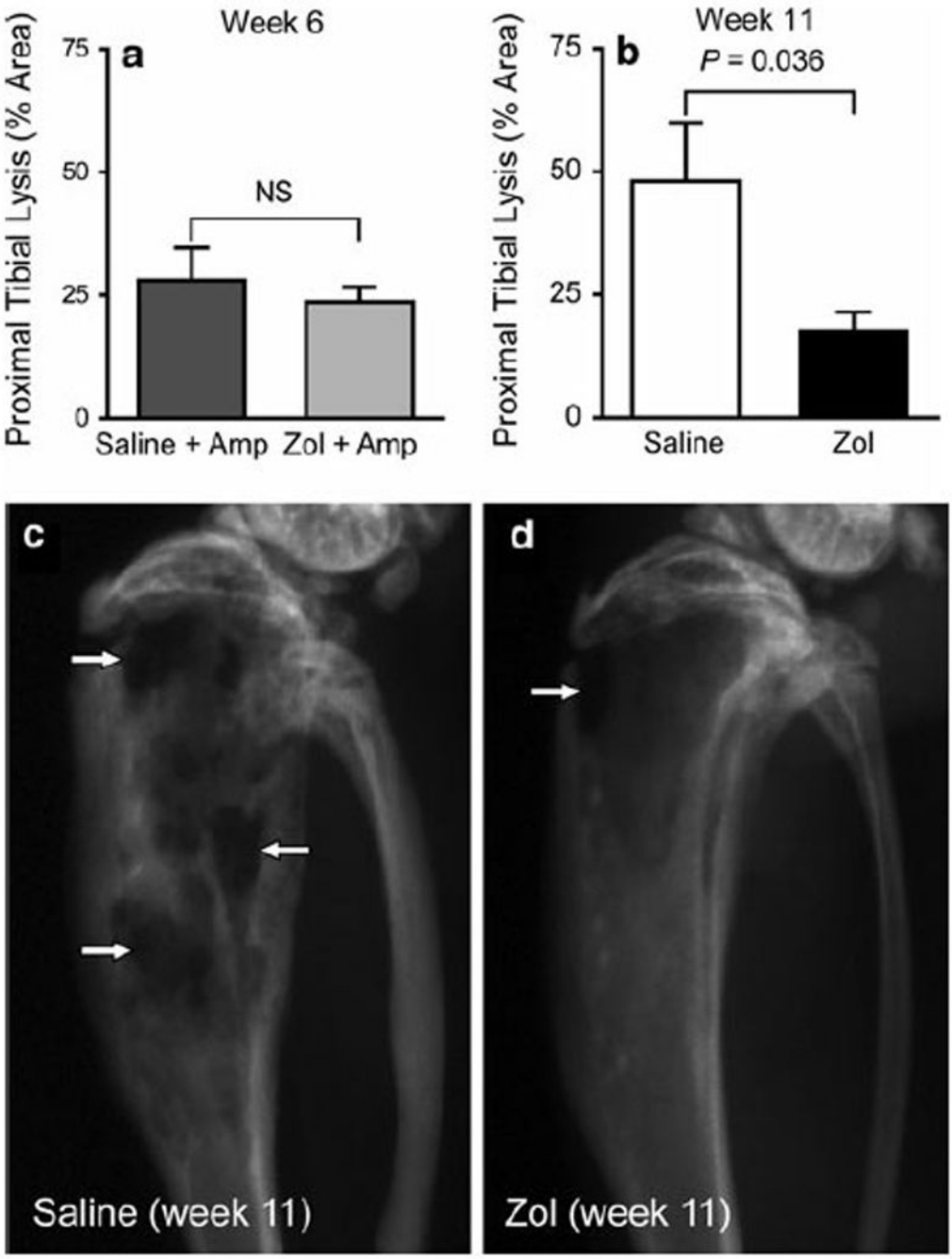

Fig. 1.

Percentage of proximal tibial lysis following Zol or saline treatment in mice injected intratibially with OSCA40 tumor cells. Tibial radiographs were taken 6 weeks after injection of tumor cells in the amputation groups treated with either saline or Zol. In the non-amputation groups treated with either saline or Zol, the radiographs were taken 11 weeks after injection of tumor cells. Percentage of proximal tibial lysis was measured as the ratio of the lytic area to the total proximal tibial area. There were no significant differences between saline and Zol-treated mice at the time of amputation at 6 weeks (**a**). In the non-

amputated mice, Zol treatment significantly reduced the percentage of proximal tibial lysis at 11 weeks (**b**). Bars represent mean ± 1 SEM of 10–12 mice per treatment group. Greater cortical and trabecular bone lysis (*white arrows*) was present in the tibial radiographs from non-amputated mice treated with saline (**c**) in comparison to the Zol-treated mice that had intact cortices with mild cortical bone loss (**d**)

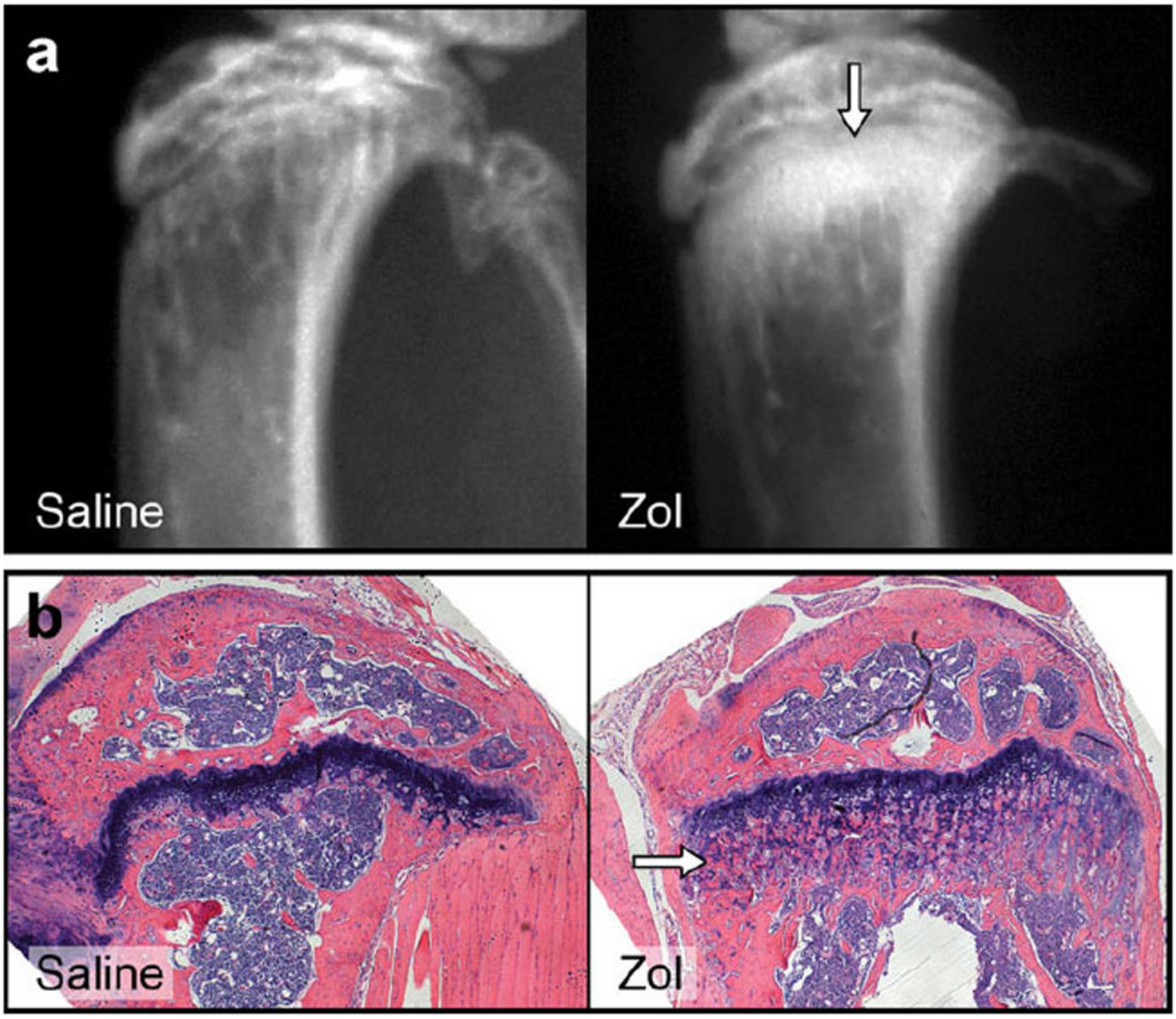

Fig. 2.

Zol-treated nontumor-bearing mice had the expected increase in proximal metaphyseal radiopacity (*white arrow*) compared to vehicle-treated nontumor-bearing mice (**a**). Histology of Zol-treated mice demonstrated increased thickness and number of primary spongiosa (*white arrow*) compared to saline-treated mice (**b**)

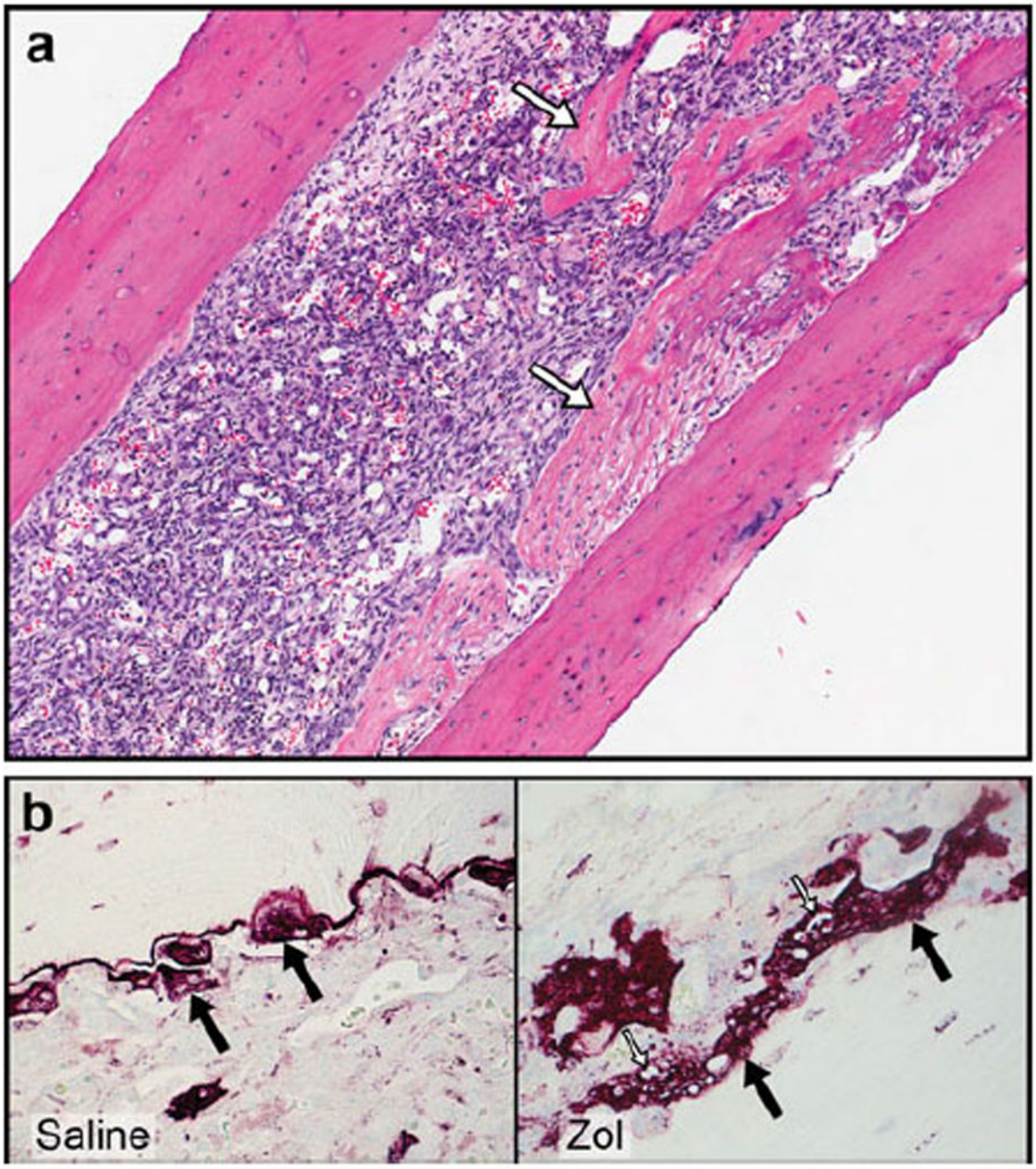

Fig. 3.

Zol treatment prevented cortical bone lysis in tumor-bearing mice and supported new woven bone formation adjacent to the lytic tumors in the metaphysis and proximal diaphysis (*white arrows* **a**). TRAP-staining revealed numerous osteoclasts (*black arrows*) along the tumor-bone interface in Zol- and saline-treated mice. In the Zol-treated group, osteoclasts were large and had cytoplasmic vacuoles (*white arrows*) when compared to the saline-treated group (**b**)

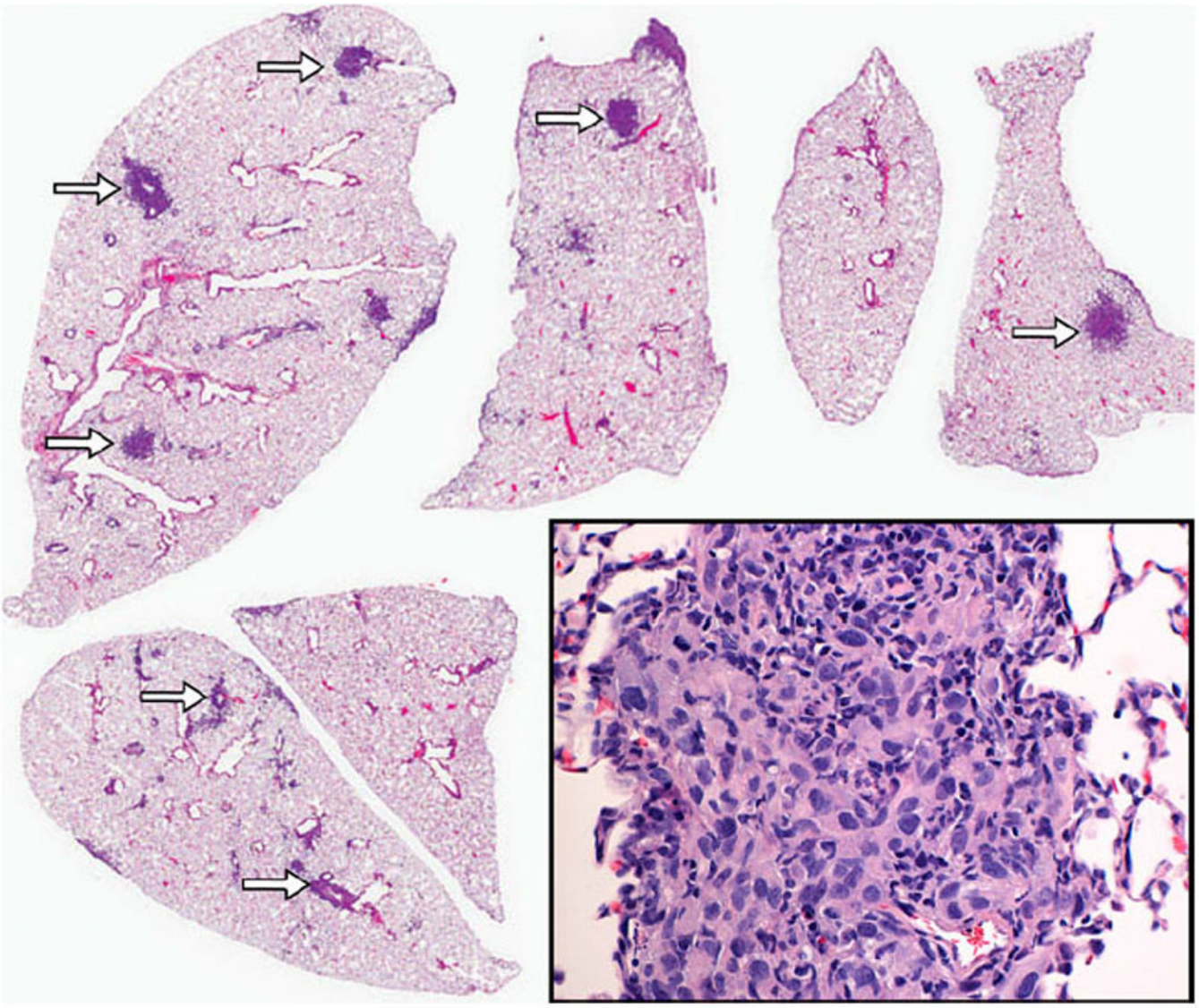

Fig. 4.

Intrapulmonary metastases of varying sizes were distributed randomly within the lung parenchyma (*arrows*). The pulmonary metastases consisted of anaplastic spindle shaped cells consistent with OSA

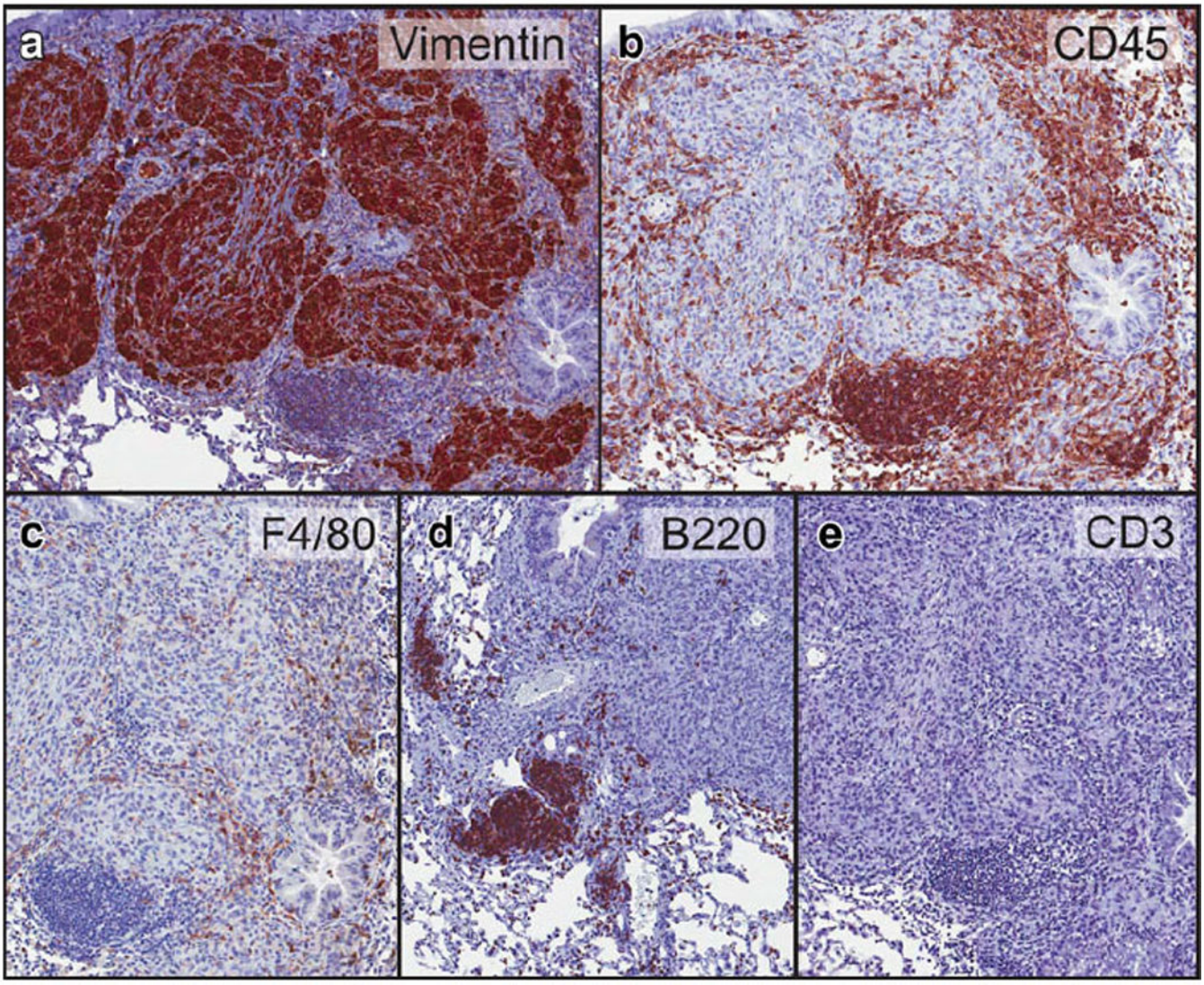

Fig. 5.

Immunohistochemistry of the lung metastases. OSA cells of the lung metastases had immunoreactivity for canine-specific vimentin (**a**). The inflammatory cells stained for a murine pan-leucocyte marker (CD45, **b**). The inflammatory cells consisted of mouse macrophages (F4/80, **c**), B-cells (B220, **d**), T-cells (CD3, **e**)

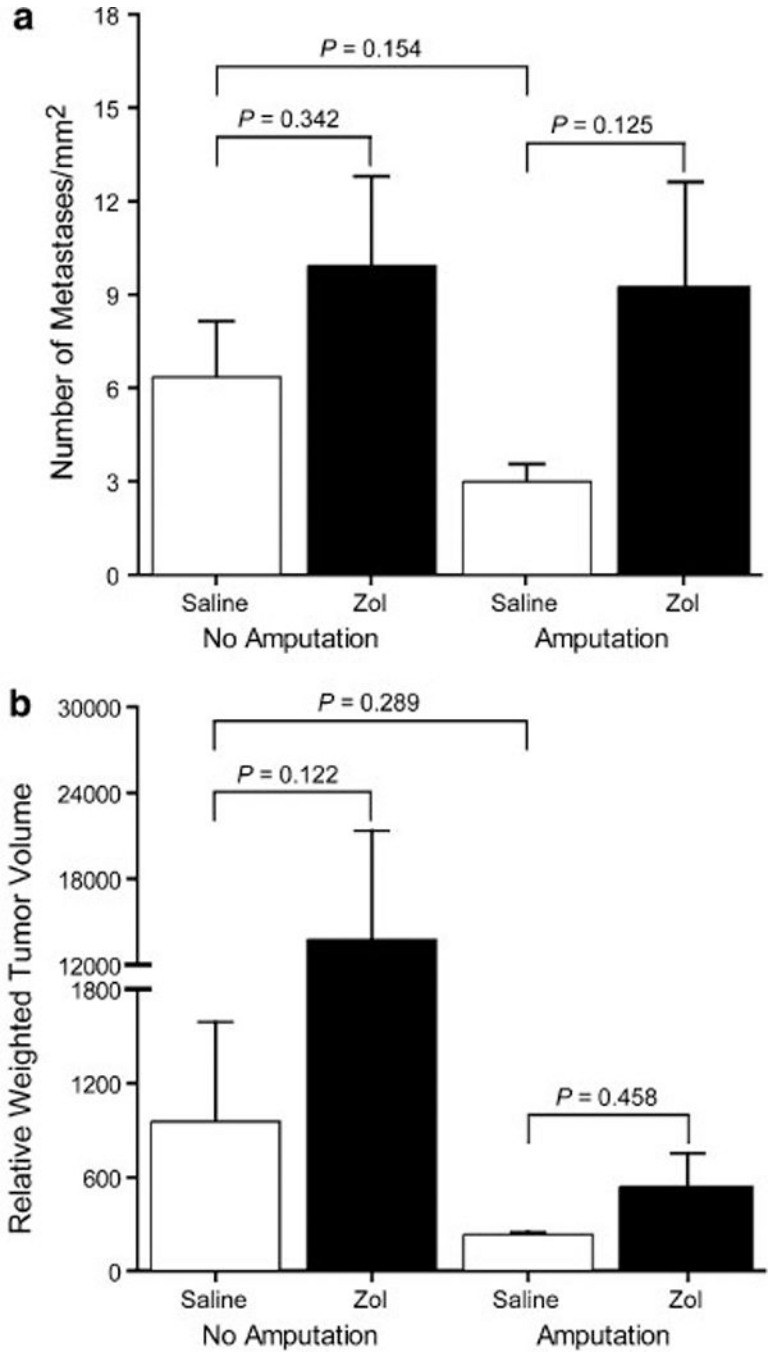

Fig. 6.

Incidence of lung metastasis (per mm^2) (**a**) and relative weighted tumor volume (**b**) in mice developing metastases. Bars represent mean ± 1 SEM. Amputation reduced the average incidence of metastasis when compared to treatment with saline alone or Zol and amputation; however, it did not result in a statistically significant difference ($P = 0.154$ and 0.125, adjusted threshold for significance $P < 0.017$, **a**). Despite an increase in average relative weighted tumor volume following Zol treatment in non-amputated mice ($P = 0.122$,

adjusted threshold for significance $P < 0.017$, **b**), there were no statistically significant differences between treatment groups

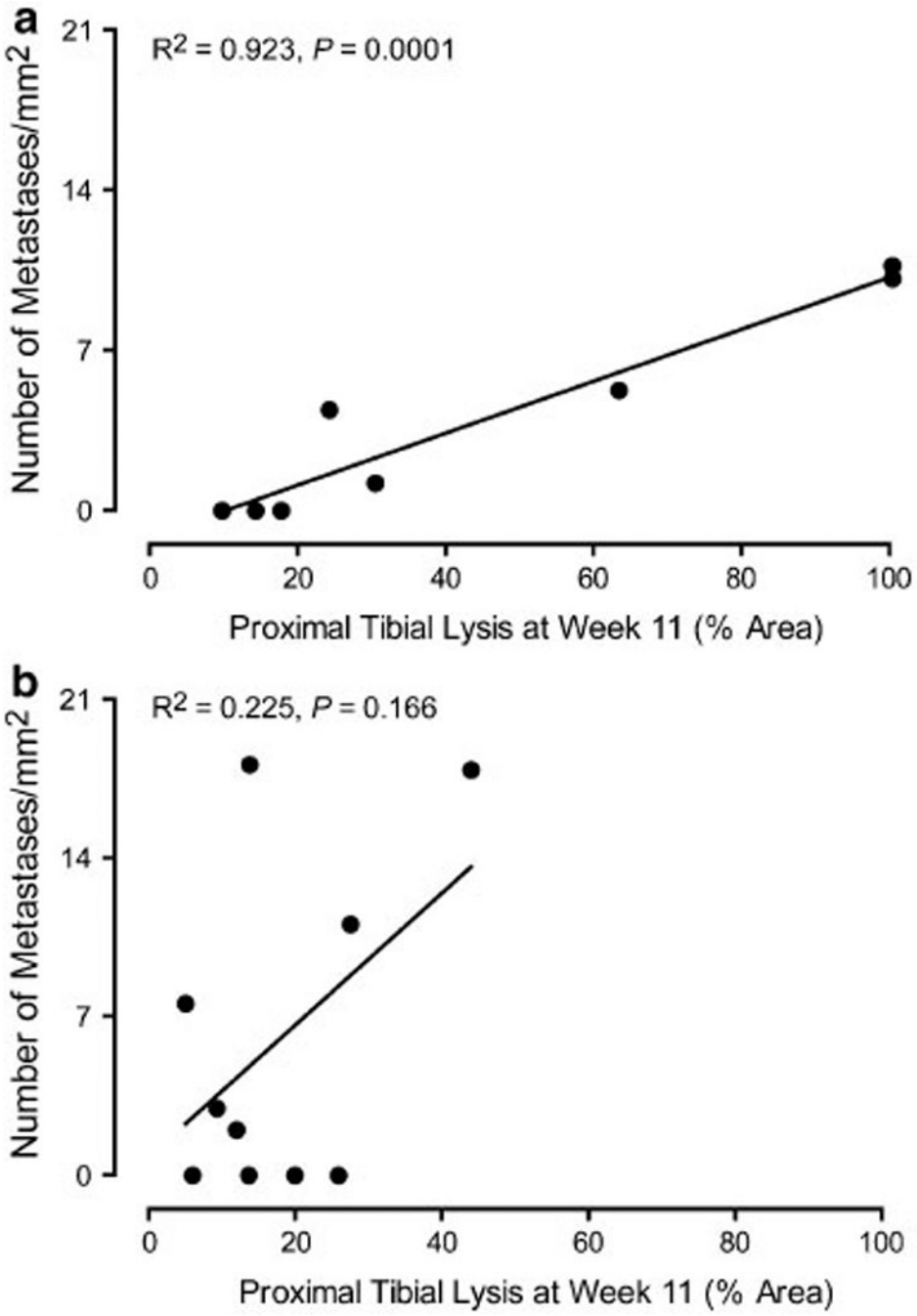

Fig. 7.

Correlation between the incidence of metastasis and percent bone lysis of the proximal tibia at week 11 in non-amputated mice treated with saline (**a**) or Zol (**b**). Pearson correlation analysis revealed a significant correlation between the incidence of metastasis and proximal tibial lysis in saline-treated mice without amputation (P = 0.0001, **a**)

Table 1

Basis for relative weighted tumor volumes for each size classification

Size classification (μm)	Midpoint diameter (μm)	Arbitrary radius value (*r*)	Arbitrary relative tumor volume ($4/3\pi r^3$)
<100	50	1	4.2
100–200	150	3	110
200–300	250	5	520
300–500	400	8	2,100
500–800	650	13	9,200
>800	1,000	20	34,000

Table 2

Antibodies used for immunohistochemistry of pulmonary metastases

Primary antibody			Secondary antibody	
Targeted antigen	**Dilution**	**Company**	**Source**	**Dilution**
Vimentin	1:100	DakoCytomation	Biotinylated Horse Anti-Mouse	1:200
B220	1:200	BD Biosciences	Biotinylated Rabbit Anti-Rat	1:100
CD3	1:1,000	DakoCytomation	Biotinylated Goat Anti-Rabbit	1:1,000
F4/80	1:100	AbD Serotec	Anti-Rat	1:200
CD45	1:500	BD Biosciences	Anti-Rat	1:100

Table 3

Incidence of lung metastasis, percentage of mice developing metastasis within each treatment group, and the relative size distribution of metastases

Treatment	Number of mice with metastasis	<100 μm	100–200 μm	200–300 μm	300–500 μm	500–800 μm	>800 μm
Saline	5 of 8 (63%)	4 of 5 (80%)	4 of 5 (80%)	2 of 5 (40%)	1 of 5 (20%)	0 of 5 (0%)	0 of 5 (0%)
Zol	6 of 10 (60%)	6 of 6 (100%)	6 of 6 (100%)	4 of 6 (67%)	3 of 6 (50%)	1 of 6 (17%)	1 of 6 (17%)
Saline + Amp	4 of 10 (40%)	3 of 4 (75%)	3 of 4 (75%)	0 of 4 (0%)	1 of 4 (25%)	0 of 4 (0%)	0 of 4 (0%)
Zol + Amp	6 of 10 (60%)	6 of 6 (100%)	5 of 6 (83%)	3 of 6 (50%)	0 of 6 (0%)	1 of 6 (17%)	0 of 6 (0%)